Virology 409 (2011) 91–101

Contents lists available at ScienceDirect

Virology

journal homepage: www.elsevier.com/locate/yviro

Capsid protein identification and analysis of mature Triatoma virus (TrV) virions and naturally occurring empty particles

Jon Agirre [a,c], Kerman Aloria [b], Jesus M. Arizmendi [c], Ibón Iloro [d], Félix Elortza [d], Rubén Sánchez-Eugenia [a,h], Gerardo A. Marti [e], Emmanuelle Neumann [f], Félix A. Rey [g], Diego M.A. Guérin [a,c,h,*]

[a] Unidad de Biofísica (CSIC-UPV/EHU), Barrio Sarriena S/N, 48940, Leioa, Bizkaia, Spain
[b] Servicio General de Proteómica (SGIker), Universidad del País Vasco (UPV/EHU), 48940 Leioa, Spain
[c] Departamento de Bioquímica y Biologia Molecular, Universidad del País Vasco (UPV/EHU), 48940 Leioa, Spain
[d] CIC-BioGUNE, Proteomic plataform, CIBERehd, Proteored, Parque Tecnológico Bizkaia, Ed800, 48160 Derio, Bizkaia, Spain
[e] Centro de Estudios Parasitológicos y de Vectores (CEPAVE) and Centro Regional de Investigaciones Científicas y Transferencia Tecnológicas La Rioja (CRILAR), 2#584 (1900) La Plata, Argentina
[f] Laboratoire de Microscopie Electronique Structurale, Institut de Biologie Structurale Jean-Pierre Ebel, UMR 5075 CEA–CNRS–UJF, 41, rue Jules Horowitz, F-38027 Grenoble, Cedex 1, France
[g] Unité de Virologie Structurale, CNRS URA 3015, Départment de Virologie, Institut Pasteur, 25 rue du Docteur Roux, 75724 Paris Cedex 15, France
[h] Fundación Biofísica Bizkaia, B Sarriena S/N, 48940 Leioa, Bizkaia, Spain

ARTICLE INFO

Article history:
Received 4 June 2010
Returned to author for revision
9 August 2010
Accepted 29 September 2010
Available online 27 October 2010

Keywords:
Dicistroviridae
Triatoma virus
VP4
VP0 cleavage
RNA encapsidation
Virus assembling
Empty capsid
Chagas disease

ABSTRACT

Triatoma virus (TrV) is a non-enveloped +ssRNA virus belonging to the insect virus family *Dicistroviridae*. Mass spectrometry (MS) and gel electrophoresis were used to detect the previously elusive capsid protein VP4. Its cleavage sites were established by sequencing the N-terminus of the protein precursor and MS, and its stoichiometry with respect to the other major capsid proteins (VP1–3) was found to be 1:1. We also characterized the polypeptides comprising the naturally occurring non-infectious empty capsids, i.e., RNA-free TrV particles. The empty particles were composed of VP0–VP3 plus at least seven additional polypeptides, which were identified as products of the capsid precursor polyprotein. We conclude that VP4 protein appears as a product of RNA encapsidation, and that defective processing of capsid proteins precludes genome encapsidation.

Introduction

Triatoma virus (TrV) is a viral pathogen of the blood-sucking reduviid bug *Triatoma infestans*, the main vector of human Chagas disease, also called American Trypanosomiasis (WHO, 2002). TrV is a member of the Cripavirus genus (type: Cricket Paralysis Virus, CrPV) in the *Dicistroviridae* family, which is a newly characterized family of small ssRNA(+) viruses of invertebrates. The dicistrovirus genome is characterized by having two open reading frames, ORF1 and ORF2, which encode the non-structural proteins and the precursor structural protein P1, respectively (ICTVdb: 00.101.). Due to the structural and taxonomical similarities between these insect viruses, comovirus plant viruses (Bonning and Miller, 2010), and picornaviruses from animals (Rossmann and Tao, 1999; Tate et al., 1999), their study will lend insight into the mechanisms of viral infection and the complex molecular events associated with non-enveloped virus capsid assembly.

Former studies on proteins extracted from purified TrV gave only four bands as analyzed by one- and two-dimensional gel electrophoresis (Muscio et al., 1988; Rozas-Dennis and Cazzaniga, 2000). Three clearly separated and roughly equimolar (1:1:1 stoichiometry) major bands at 39 kDa (VP2), 37 kDa (VP1) and 33 kDa (VP3) were observed along with a minor band of about 45 kDa (VP0), which appeared as a doublet when stained with silver nitrate (Muscio et al., 1988). As with CrPV (Moore et al., 1980) and the aphid virus *Rhopalosiphum padi* of the same virus family (Williamson et al., 1988), in TrV the low molecular mass protein VP4 could never be identified by gel electrophoresis (Muscio et al., 1988), and therefore its N-terminal sequence remained unknown. Based on sequence alignment with other cripaviruses two possible putative cleavage sites were assigned leaving VP4 with a theoretical mass of either 5.5 kDa or 4.4 kDa (Czibener et al., 2000).

When the crystallographic structure of CrPV was solved, a clear electron density at the capsid interior allowed VP4 protein to be easily identified as a constituent of the virus capsid (Tate et al., 1999). Recently, we determined the crystallographic structure of TrV (Squires et al., in preparation; PDB ID: 3NAP). While this structure is remarkably similar

* Corresponding author.
E-mail address: diego.guerin@ehu.es (D.M.A. Guérin).

0042-6822/$ – see front matter © 2010 Elsevier Inc. All rights reserved.
doi:10.1016/j.virol.2010.09.034

to that of CrPV, the lack of electron density in TrV structure attributable to VP4 protein is a surprising difference between the two viral capsids. Although many picornavirus structures lack VP4, it is well accepted that in this vertebrate virus family the final virion maturation step requires the partition of VP4 from VP0 (Basavappa et al., 1994), and that VP4 also plays an important role during cell infection (Brabec et al., 2005; Tuthill et al., 2006). For these reasons, when the CrPV structure came to light, it was speculated that VP4 might play a similar role in cripaviruses as it does in mammalian picornaviruses (Rossmann and Tao, 1999).

The uncertainty about VP4 protein in TrV made us suspicious about the effectiveness of the methods so far employed to analyze the capsid proteins of this virus. Therefore, one of the main goals of this study was to establish whether or not VP4 is a component of mature, fully processed TrV virions.

In a former study on TrV using transmission electron microscopy (TEM), we reported that in fresh purified TrV samples a mixed population of RNA-containing (*full*) and RNA-free (*empty*) virus capsids is always observed, in addition to smaller particles (Estrozi et al., 2008). This result led us to suspect that the protein composition of different TrV particles might be heterogeneous. Also, we were intrigued about the nature of the empty capsids, whether they had already delivered their RNA or they had been unable to encapsidate the genome. To address these issues, we improved the current purification method and successfully separated the different TrV components; empty particles were purified and separated away from the predominant full virus population, and their respective protein composition was analyzed by MS. Similarly to what happens in full virions, our results showed that empty capsids contain VP0–VP3 proteins. However, in contrast to full capsids in which VP3 protein is one of the major components, in empty particles this protein is present at a lower concentration with respect to VP1 and VP2. Moreover, we found that at least seven additional polypeptides with both lower and higher MWs than VP0–VP3 are integral components of empty TrV capsids. Also, in empty particles the polypeptide precursor of VP4 and VP3, VP0, appears at higher concentrations than in full particles. More importantly, both MS and gel electrophoresis unequivocally identified the putative small VP4 protein as a component of full virions, establishing both its length and amino acid composition. All these results serve to better characterize TrV particles, and the implications for genome encapsidation are discussed.

Results and discussion

Virus purification

In all former studies on TrV, the purification protocols used whole bodies and/or the intestinal portion of infected triatomine insects as the source material (Marti et al., 2008; Czibener et al., 2005, 2000; Rozas-Dennis et al., 2004, 2002, 2000; Muscio et al., 1997,1988, 1987). In this report, we used dry feces from TrV-infected insects as the primary virus source. From this source we were able to reach yields of about 0.25 mg of virus per gram of starting material. This procedure for TrV purification is advantageous because it avoids the handling of dead and/or living insects, it does not require sacrificing the insectary's population, and it allows fresh virus to be obtained from material that does not require special storage and/or transport conditions.[1] Additionally, using the excrement of TrV-infected insects allows the virus production from a laboratory colony to be optimized, because TrV can be purified from insects throughout their life without causing any damage due to sample extraction. Feces can either be extracted as fresh material by abdominal compression immediately before insect feeding, or later by harvesting from the rear vessel as dry buttons.

TrV was usually extracted from both CsCl and sucrose gradients as an apparently homogeneous single band as observed under UV light, a band that corresponded to a sedimentation coefficient of about 165 S (Muscio et al., 1988; Rozas-Dennis, et al., 2004). Muscio and collaborators observed that empty and full particles differ slightly in buoyant density and have a mean value of ca. 1.39 g/mL; therefore, the two particle species migrate very closely in a standard CsCl gradient (Muscio et al., 1988). This is in contrast to what happens with the picornaviruses foot-and mouth disease virus (FMDV; Rowlands et al., 1975), poliovirus (PV; Basavappa et al., 1994) and rhinovirus 14 (HRV14; Lee et al., 1993), in which full particles have a buoyant density of about double that of the corresponding empty particles.

Aiming to separate the two TrV particle species, in the present study we improved the previously reported purification method by introducing two novel steps. At the beginning of the protocol and after maceration of the starting material, a few minutes of sonication was included to disaggregate the mixed virus and capsid clusters. The second variation to the current protocol was to increase the relative centrifugal force up to 180,000 g_{avg} during the second pre-processing centrifugation. This modification caused the empty particles to pellet together with the full virions. Once the pellet was resuspended the material was loaded into a continuous 5%–30% sucrose gradient and run at 100,000 g_{avg} for 3 h. Then, the gradient was fractionated from the bottom to the upper part into small (0.5 mL) aliquots, and by measuring the UV absorbance of each fraction at both 260 nm (accounting for peak RNA absorbance) and 280 nm (accounting for peak amino acid absorbance), the two particle species could be separated (Fig. 1). In fact, the relative absorbance intensity between the two UV wavelengths varied across the elution depending on the RNA/amino acid content. This fact is apparent in Fig. 1A, in which the curve marked with circles corresponds to the OD_{260}, and that marked with triangles corresponds to the OD_{280}. The big peak (fractions 7 to 22) had higher absorbance at 260 nm than at 280 nm, indicating a gradient region with higher RNA content. The protein composition of the samples belonging to this region shows three clear major bands corresponding to VP1–3 and a barely visible VP0 band (Fig. 1B). The peak is mainly composed of full TrV virus (see below), and after background correction the average OD_{260nm}/OD_{280nm} ratio ≈ 2. A second region corresponding to aliquots 31 through 39 had a mean OD_{260nm}/OD_{280nm} ratio $= 1$.[2] This gradient region contained a particle population richer in empty TrV capsids (see below). The top fractions with numbers above 40 showed low protein content and higher heterogeneity than those observed within the peak and aliquots 31–39.

Dynamic light scattering (DLS) analysis

We employed DLS measurements (Schmitz, 1990) to determine the particle size (the *hydrodynamic diameter*) of the constituents of each sucrose gradient fraction. In Fig. 1, the results obtained for seven representative gradient fractions are shown. In this figure, the DLS measurements are indicated as marks on top of dashed vertical segments. The size indicated as $Peak_1$ corresponds to the centroid of the particle size distribution of the most abundant particle population, that of the second most abundant particle population to $Peak_2$, and so forth. Each hydrodynamic diameter is shown and is separated by a '/'

[1] Serological studies of Chagas' disease patients living in endemic areas of high incidence of naturally occurring TrV infection indicate that no anti-TrV antibodies could be found in sera (Czibener et al., 2000; Muscio et al., 2000). Since TrV is infective within insect feces (Muscio et al., 2000), millions of humans, goats, sheep and domestic animals like dogs and cats have already been exposed to TrV without showing viral replication. For this reason, TrV can be considered to be unlikely to cause human disease, and according to the directive 2000/54/EC of the European Parliament and of the Council (September 18, 2000), it is to be classified as a Risk Group 1 biological agent, with no identifiable health risk to workers. According to this directive, no special safety measures have to be taken for working with TrV but 'the principles of good occupational safety and hygiene should be observed.'

[2] Although the absorbances corresponding to that particular peak are close to the background, dialyzed and thereafter concentrated samples of empty capsids show the exact same absorbance ratio.

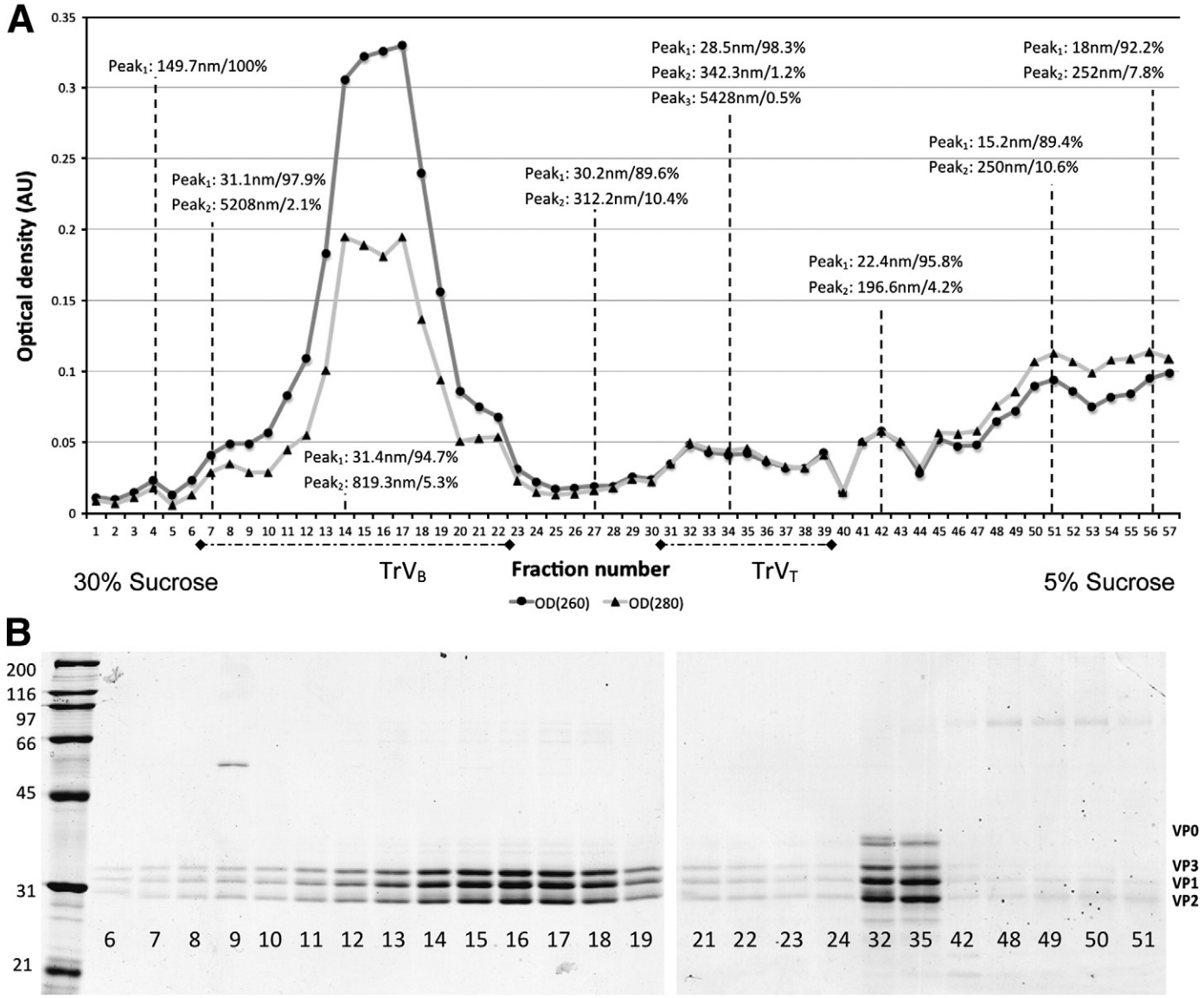

Fig. 1. A. Continuous 5%–30% sucrose gradient analysis. Fractions collected were numbered from 1 (bottom section of the tube) to 57 (upper region of the tube). The circle-marked and triangle-marked curves correspond to the optical absorbance measured at 260 nm and 280 nm, respectively, and for both lines a major peak exists that corresponds approximately to the region between fractions 7 and 22. This gradient region (TrV_B) contains RNA-full TrV capsids, while an empty particle population appears between fractions 31 and 39 (TrV_T), as indicated by the relative increase in absorbance at 280 nm. Representative gradient fractions were analyzed by means of DLS (dashed vertical segments). This analysis allows to measures the particle size distribution centroid corresponding to the most abundant dispersing particle population ($Peak_1$) and its relative abundance (in % values) with respect to the second most abundant particle population ($Peak_2$). B. 12.5% polyacrylamide gels show the protein composition of several gradient fractions (numbers 6–19, 21–24, 32, 35, 42, 48–51). The VP0–VP3 labels indicate the band positions corresponding to the four representative TrV capsid proteins. The band patterns in samples 32 and 35 are characteristic of empty particles due to the high VP0 protein content. The numbers in the column at the left indicate MW references in kDa.

from the percent relative abundance (referred to as the volume of the dispersing sample). As expected, the biggest particles, most likely to be contaminants or TrV aggregates, migrated to the bottom of the gradient (fraction 4). The peak region (TrV_B) had particle size values very close to 30 nm, which corresponds to the geometrical size of TrV virions. The DLS measurements in the TrV_T region also indicated a major population (98%) of particles sizing about 30 nm. From the particle size observed at the top of the gradient (fractions 51 through 56) we can presume that most of the dispersing material comes from disassembled virus (protein and/or RNA).

Transmission electron microscopic (TEM) analysis

When analyzed under an electron microscope, TrV samples obtained after the first pre-processing step showed a mixture of RNA-full and empty capsids, as well as many variously shaped small particles, some of them with pentameric symmetry (Fig. 2A). A previous study (Estrozi et al., 2008) in which a model-free 3D EM reconstruction was performed at about 25 Å resolution showed that the main difficulty in improving the resolution came from the particle mixture present in the samples. In this study we found that the reconstructed TrV capsid was thinner than the resolved crystallographic structure, and this discrepancy might also be attributable to state of the particles: empty or full, respectively. When TrV was separated through a continuous 5%–30% sucrose gradient, the two collected samples (TrV_B and TrV_T) were composed of two different particle populations: the bottom fraction (TrV_B) had an almost homogeneous population of RNA-full TrV particles (Fig. 2B), whereas the top fraction (TrV_T) had a mixture of very few RNA-full particles, a major population of empty TrV capsids and an intermediate population of small particles (Fig. 2C). Interestingly, the small particles appeared

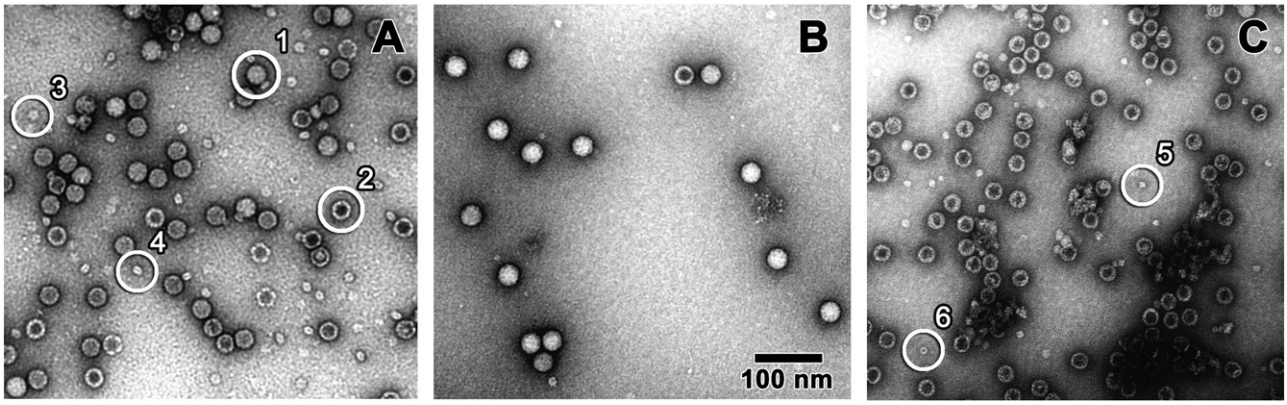

Fig. 2. Stained-TEM images of TrV particles. A. TrV particles obtained after the first purification step and dialyzed against NMT buffer. Mixtures of full virions (1), empty particles (2), and most likely capsid disassembly intermediates appearing as small particles with either pentameric (3) or dimeric symmetry (4) are visualized. B. The bottom peak fraction (TrV_B) is composed of a major population of full TrV particles. C. The top gradient fraction (TrV_T) contains a mixed population of 30-nm empty TrV capsids (disks with black centers), very few full particles (homogeneous disks) and small particles most likely arising from capsid disassembly (5 and 6).

within the peaks of the gradient. Because the size of these particles was much smaller than either empty or full capsids, it is plausible to speculate that these small particles did not co-migrate with the capsids but rather are disassembly products of empty particles. If so, and because no small particles were present in the images of the TrV_B fraction, this should indicate that under our experimental conditions mature virions (i.e., particles containing RNA) are more stable than empty TrV capsids.

Infectivity of empty TrV particles

In order to verify the non-infectivity of empty capsids, we conducted experimental infection tests with healthy *T. infestans* insects as described in Materials and methods. Insects inoculated with infective TrV particles died within 24 h after inoculation, whereas 20% mortality was observed in the control group (using sterile saline solution as the inoculum). A corrected mortality of 0% was observed in the two insect groups inoculated with NMT buffer and empty TrV particle solution (data not shown). Because empty particles are not infective whereas purified TrV is lethal when injected intra-hemocoelically (Muscio et al., 1997), these results confirm that empty TrV particles lack the viral genome.

Polyacrylamide gel electrophoretic analyses

Previous SDS-PAGE analyses of TrV (Muscio et al., 1988) showed that the bigger TrV capsid proteins could be separated employing standard *Laemmli* loading buffer containing β-mercaptoethanol for disulfide bond reduction. In the present study, we employed loading buffer both with and without β-mercaptoethanol with identical results in the separation of the proteins (data not shown), indicating that no disulfide bridges are formed between the five cysteines present in the three major capsid proteins (VP1–VP3).

SDS-PAGE analysis of the TrV_B and TrV_T fractions gave two different polypeptide patterns (Fig. 3A). The sample with $OD_{260} > OD_{280}$ (TrV_B) showed three clearly separated major bands named VP1–3, VP0, a minor band of lower electrophoretic mobility that corresponds to the putative polypeptide precursor of VP4 and VP3, and a thin band/polypeptide (PP) named PP3 (Fig. 3A, left line). The three polypeptides with higher mobility correspond to TrV capsid proteins VP3, VP1 and VP2, with theoretical masses of 31.9, 29.7, and 28.5 kDa, respectively. The slowest band corresponds to protein VP0 with an electrophoretic mobility of 38 kDa. These results are consistent with the initial characterization of TrV capsid proteins, including the band PP3 that was previously reported as part of a doublet of VP0 that appeared in several virus preparations purified from CsCl gradients (Muscio et al., 1988).[3] These authors reported a value of 1.8 for the OD_{260}/OD_{280} ratio, which is lower than what we observed in the TrV_B peak ($OD_{260}/OD_{280} = 2$). This difference can be attributed to the higher RNA content of the TrV_B samples as a consequence of the depletion of empty TrV capsids.

Fractions belonging to the TrV_T region (with $OD_{260} \approx OD_{280}$) contained the same band pattern as those from TrV_B plus at least seven additional polypeptides (Fig. 3A, central line). The major bands corresponded to the VP1 and VP2 proteins, and VP0 and VP3 were intermediate bands. In addition to these TrV capsid proteins, we identified seven additional bands named PP0 to PP6; PP3 and PP4 were of intermediate intensity, and the others were of weak intensity. We refer to these polypeptides/bands as *non-canonical* proteins (i.e.: PP0–PP6), and they were further characterized by MS and N-terminal sequencing. Since almost all the non-canonical proteins come from the polypeptide capsid precursor (see below), we deduced that empty capsids were unable to encapsidate the genome due to the loss of specific interactions between the RNA and the capsid proteins, most likely as a consequence of misprocessing of the protein precursor P1. Interestingly, despite the flawed processing of P1, the specific interactions driving capsid assembly are still retained. As has been previously observed in other icosahedral viruses (Salunke et al., 1989; Iwasaki, et al., 2000; Ceres and Zlotnick, 2002; Johnson et al., 2005; Siber and Podgornik, 2007), this result indicates that in TrV the genetic material is not necessary for capsid assembly.

Densitometric analysis of capsid proteins separated by gel electrophoresis

Densitometric analysis of the gel bands (Fig. 3A) corresponding to the electrophoretic pattern of the gradient fractions TrV_B and TrV_T is shown in Table 1. Analogously to what is observed in CrPV and model picornaviruses, we presume that in TrV the *ideal* virus capsid is built of 60 identical protomers, with each protomer made of VP1–VP4. Even though the TrV_B fractions had some contamination with empty capsids,

[3] Initially, Muscio et al. (1988) named the TrV capsid proteins VP0–VP4 analogously to rhinovirus proteins. According to this scheme, VP0 should be the precursor of VP4 and VP2. Later, when the genome of TrV was sequenced (Czibener et al., 2000), the genomic order of the TrV capsid proteins was assigned as VP1, VP4, VP2 and VP3, encoded respectively at the 5′ and 3′ ends of the ORF2 (nucleotides 6109–8715). We renamed VP1–VP3 proteins analogously to the structural proteins of CrPV, the prototypic virus of the *Dicistroviridae* family (Tate et al., 1999), VP0 being the precursor of VP4 and VP3, and VP2 and VP1 encoded respectively at the 5′ and 3′ ends of ORF2.

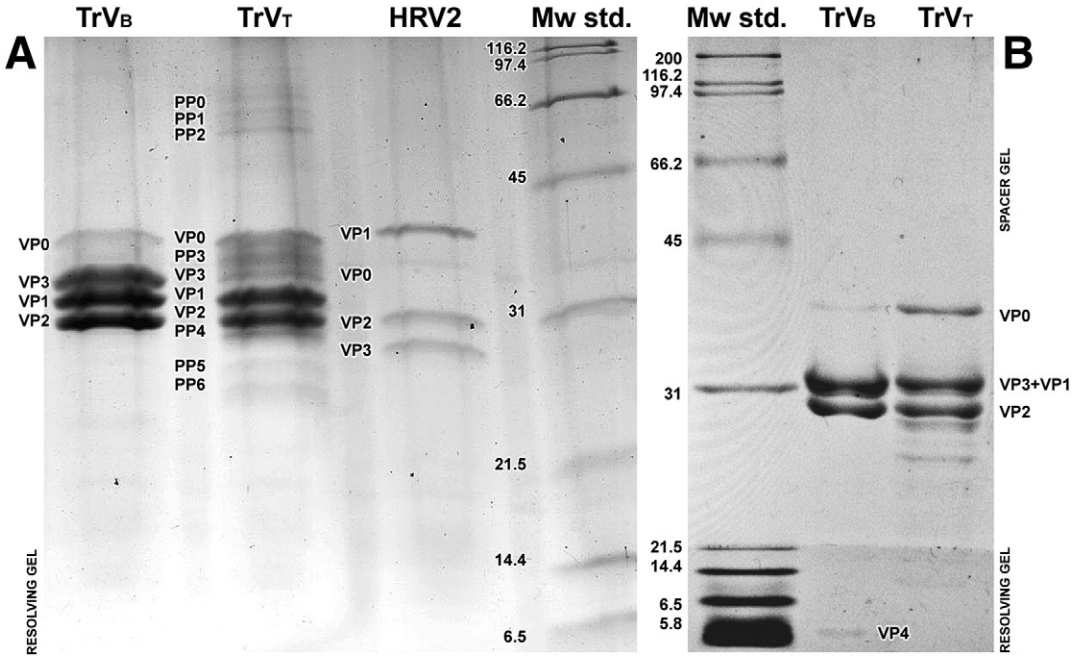

Fig. 3. SDS-PAGE analyses of TrV proteins. A. TrV_B and TrV_T fractions (10 μL) (Figs. 2B and C respectively) were run in a 15% polyacrylamide gel giving the polypeptide patterns of line 1 and line 2, respectively. HRV2 (line 3) was included as a reference. In full TrV particles (TrV_B), five proteins were detected: VP0–VP3 (Muscio et al., 1988) and a thin band named PP3 located between VP0 and VP3, which may account for the doublet reported. For TrV_T (empty capsids), a more complex polypeptide pattern appeared: all proteins making up the full particles were also present, but their relative weights varied, with VP3 as a minor component and the levels of VP0 and PP3 increased. Additionally, at least six other bands indicate that more proteins form part of these empty particles. These bands were identified as PP0–6. B. Using a custom Tris–Tricine 15% acr./bisacr. (48:3) separating gel, it was possible to detect by electrophoresis the small capsid protein VP4 in TrV_B samples. Gels were stained with Coomassie blue for quantitative analysis in order to determine band stoichiometry.

summing up the values corresponding to VP1–VP3 from the percentage values of Table 1 column 2, we see that 93.6% of the structural proteins are correctly assembled. The same analysis of the TrV_T fractions indicated that about 40% of the capsid proteins were incorrectly folded and/or had longer or shorter chains than the canonical VP1–VP3 proteins.

It was previously reported for mammalian picornaviruses that the protein precursor VP0 is one of the major components that make up empty capsids (in Poliovirus: Basavappa et al., 1994; Jacobson and Baltimore, 1968; in Foot and Mouth Disease Virus: Rweyemamu et al., 1979; Rowlands et al., 1975). Similarly to what happens in picornaviruses, we found that in TrV VP0 appears at higher concentrations in empty capsid populations than in mature virus populations, and this fact led us to sequence its N-terminal region (see below). Moreover, we observed that the non-canonical polypeptides PP0–PP6 constitute in total about one-third (27.2%) of the protein content of empty capsids. A possible explanation for this phenomenon could be that the structural proteins (to be cut from P1) are expressed in stoichiometric excess relative to the non-structural ones (helicase, protease and RNA-dependent RNA-polymerase) during replication, allowing for the correct processing of just a subset of them (Tate et al., 1999).

Since there was no attributable electron density for VP4 in the crystallographic structure (PDB ID: 3NAP) and basic detection methods failed to establish its existence (Muscio et al., 1988; Czibener et al., 2000), we employed a battery of methods in order to find and eventually characterize it. Since we also were unable to resolve VP4 even in high-percentage polyacrylamide gels, we opted for a custom Tris–Tricine–SDS gel (see Materials and methods). As can be seen in Fig. 3B, in the TrV_B sample VP0, VP2 and VP4 are well-resolved, while VP3 and VP1 appear as a single, more intense band. In the case of TrV_T, we were unable to identify VP4 even after the gel was stained with silver nitrate (data not shown), a fact that, when compared to the well-resolved VP4 band of the TrV_B sample in the same gel, indicates that most VP4 remains as part of VP0 in empty capsids.

Quantification was performed with each of the gel bands (Fig. 3B) in TrV_B in order to get an estimation of the stoichiometry of VP1–VP4. Due to insufficient separation between VP3 and VP1, VP1–VP3 were treated as a single band, with an integrated optical density (IOD) of 1,367,896 (arbitrary units) and a scaled density (see Materials and methods) of 10,058. The IOD for VP4 was 40,615, leaving a scaled density of 10,153. As for VP0, the IOD was 41,876 and the scaled density was 722. Based on these results, we can infer that the processed capsid proteins (VP1–VP4) are roughly equimolar, while VP0 is in stoichiometric minority. One explanation for the presence of this precursor protein in a full virus sample could be a slight contamination from empty capsids (richer in VP0), which the sonication process was unable to disaggregate from full viruses. Another possibility is that, since we have already demonstrated that the non-cleavage of VP0 does not inhibit the formation of a full capsid, some copies of VP0 may be present in RNA-containing particles.

Table 1
Densitometric analysis of TrV capsid protein bands (Fig. 3A). The band names in column 1 are listed in the same order that they migrate in the gels (fastest at the bottom). Columns 2 and 3 indicate the optical density (OD) values (in percentage) corresponding to each protein band as resolved by 15% SDS-PAGE for the TrV_B peak and the TrV_T region of the continuous 5%–30% sucrose gradient (Fig. 1). The '–' sign indicates that the polypeptide/band was not observed in the corresponding sample.

Peptide	Band densitometry (%)	
	TrV_B	TrV_T
PP0	–	<1
PP1	–	2.5
PP2	–	2.2
VP0	4.4	10.7
PP3	2.0	10.3
VP3	27.2	7.5
VP1	34.5	29.4
VP2	31.9	25.2
PP4	–	8.2
PP5	–	1.4
PP6	–	1.6
VP4	–	–

Either way, the quantitative difference in the protein composition of the full and empty particles shows clearly that cleavage of VP0 is part of the maturation process of TrV particles, and that its cleavage is somehow prevented if the RNA has not been incorporated inside the capsid. The presence of VP0 copies in mature virus particles would explain the lack of density for VP4 in the crystallographic structure, since the coexistence of structurally similar but nevertheless different protein species (VP0 *versus* VP4 and VP3) in a crystal has a negative impact in data quality coming from the affected regions.

N-terminal sequences of VP0 and the non-canonical capsid proteins

In contrast to what happened in a previous TrV sequencing effort (Czibener et al., 2000), we were able to obtain VP0 protein in sufficient quantity from the TrV_T (empty capsid) sample to perform sequencing. In addition to VP0, out of all the non-canonical capsid proteins we were also able to transfer PP4 to a PVDF membrane, thus allowing us to perform Edman degradation with these two polypeptides. The N-terminal sequence we obtained for VP0 ('AGKE') showed unambiguously that the cleavage site between VP2 and VP0 is IVAQ/AGKE, conferring to VP0 theoretical masses of 37.3 (Fig. 4). The previously described N-terminal sequence of VP3, SKPLTT (Czibener et al., 2000) confers VP4 a theoretical mass of 5.5 kDa, which was later confirmed by MS. In the case of PP4, it seems that the gel band corresponds to a mixture of closely migrating species, yielding several amino acids for each hydrolysis step, and two plausible N-terminal sequences of four amino acids were coincident with the capsid protein precursor P1. The two sequences obtained are 'VADA' and 'VVDA'.

Mass spectrometric analysis of TrV capsid proteins

The bands obtained from the TrV_T fractions (Fig. 3A) were in-gel digested with trypsin and the resulting peptides were analyzed by MALDI TOF MS. Five (PP1–PP5) out of seven protein bands were unambiguously identified by peptide mass fingerprinting as capsid protein precursor P1 (NCBI: NP_620563, data not shown). The two proteins that did not achieve a significant score showed peptides matching the mentioned capsid protein precursor. These proteins appear to be misprocessed forms of P1, which when incorporated to a capsid prevent further particle developments.

Notably, a peptide of 852.477 m/z was observed among the matched peptides when the VP0 band was analyzed. This corresponds to a tryptic fragment from position 284 to 291 of the amino acid chain coded by TrV ORF2 (Fig. 4). To further validate this finding, we performed a MALDI TOF/TOF tandem mass spectrometric analysis of this particular peptide. The resulting tandem mass spectrum matched the same portion of the capsid protein precursor with a Mascot Score of 35 (individual ion scores greater than 32 indicate identity or extensive homology ($p<0.05$)). Therefore, we can unambiguously conclude that the sequence GFFPSIGK is part of the VP0-TrV protein precursor.

Mass spectrometric identification of VP4-TrV capsid protein

In order to confirm the existence of the putative small capsid protein VP4 as one of the structural proteins of full TrV virus particles (see Fig. 3B), a fraction of TrV_B was subjected to MS analysis. For this purpose, the mass range 4–40 kDa was selected for raw data de-convolution (Fig. 5). Surprisingly, the main peak observed corresponded to a mass of 5502.5 Da and its +22 Da sodium adducts, while the peaks corresponding to VP0, VP1, VP2 and VP3 were not detected. Problems with sample solubilization (see Materials and methods section) and low ionization efficiency could be some of the reasons to explain this result. The 5502.5 mass matched with the theoretical mass (0.84 Da error) of the TrV capsid protein precursor fragment between amino acids Ala256 and Phe312 (see Fig. 4). To further confirm the presence of this protein in the analyzed sample, we decided to top-down sequence the $[M+4\,H]^{+4}$ ion with m/z 1376.8 corresponding to the most intense ion of the 5502.5 Da protein. The protein was fragmented by argon collision-induced dissociation (CID) and the masses of the fragments were measured by tandem MS. Comparison of the experimentally

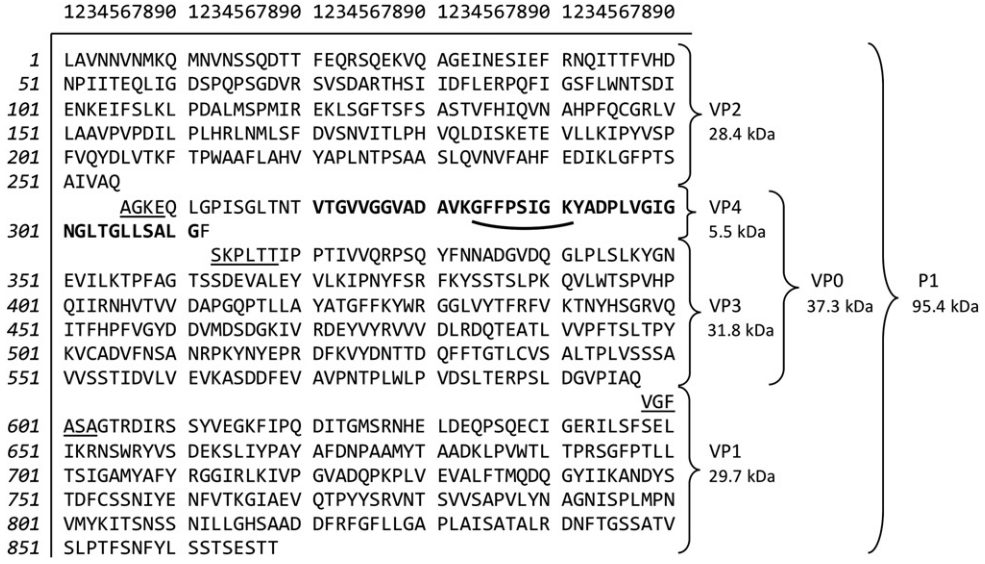

Fig. 4. Mass spectrometric analyses of VP0 and the non-canonical capsid protein components. The complete sequence corresponds to structural proteins as encoded by the TrV ORF2 viral genome (nucleotides 6109–8715; Czibener et al., 2000). The amino acids underlined correspond to the known N-terminal sequences obtained by Edman degradation. 'AGKE' marks the N-terminus of VP0 (the protein precursor of VP4 and VP3), which is predominantly present in naturally occurring empty capsids. This result, together with the known N-terminal sequence of VP1 protein as 'VGFASA,' as well as 'SKPLTT' from VP3 (Czibener et al., 2000), implies that VP0 has a theoretical mass of 37.3 kDa, while VP4 (letters in bold) is left with 5.5 kDa, an estimate that was confirmed by the MS results. The sequence portion underlined with an arc corresponds to the tryptic peptide analyzed by MALDI TOF/TOF tandem MS. The fragmentation spectrum unambiguously matched the GFFPSIGK peptide after Mascot search engine analysis. Also, from right to left, the known cleavage steps are shown, yielding as products the proteins noted by the curly brackets. First, P1 is expressed; after that, VP2, VP0 and VP1 are cut from it. The final maturation step is assumed to be the separation of VP4 and VP3.

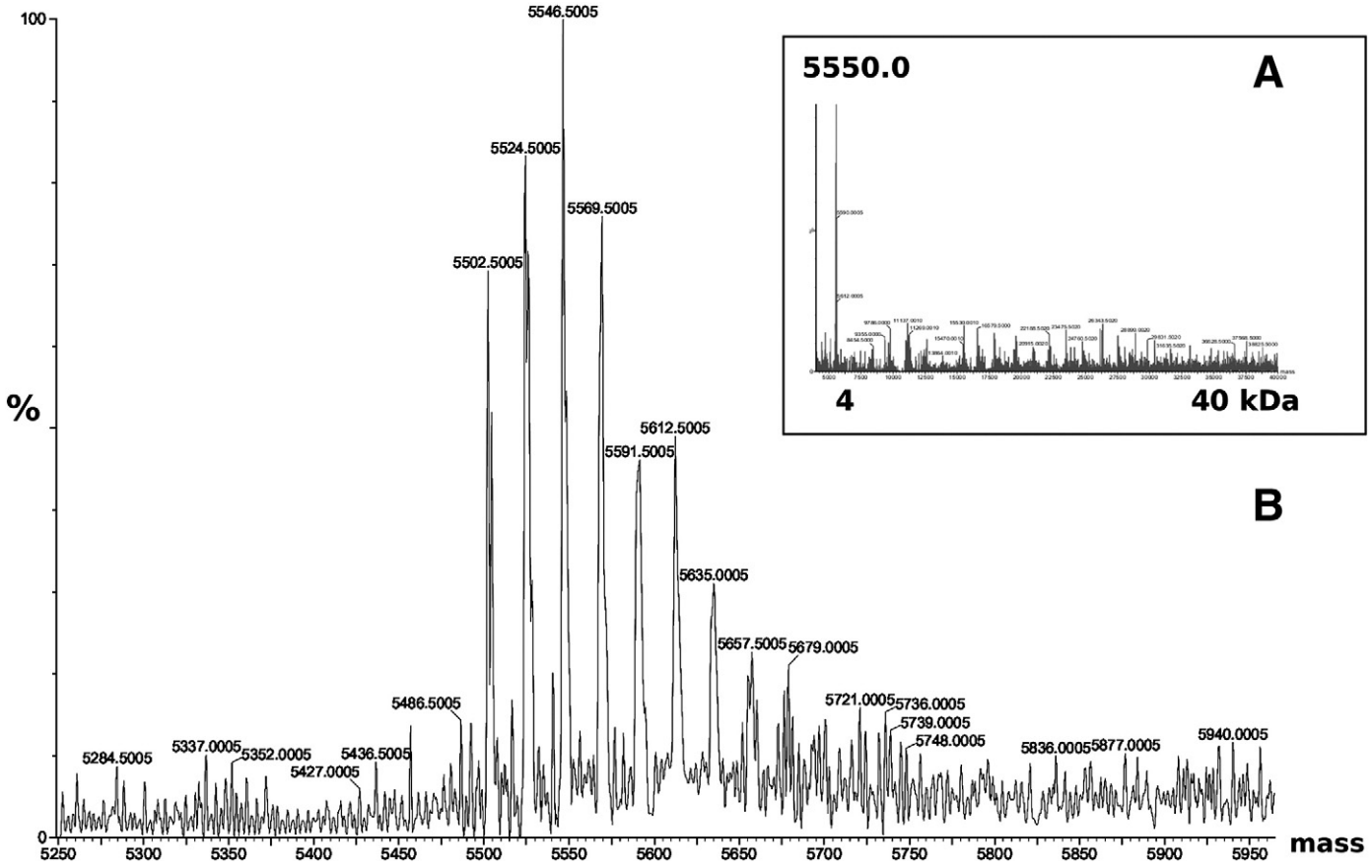

Fig. 5. Mass spectrometric analysis of an 80 μg TrVB fraction. A. Mass spectra were manually acquired in the 700–2500 m/z range. Raw data were deconvoluted between 4–40 kDa showing a major peak centered at 5550 Da. B. Zoom shot of the 5.2–5.9 kDa region in A. A mass of 5502.5 (corresponding to the mass of the putative VP4 protein minus 0.84 Da) and its +22 Da sodium adducts are resolved.

obtained fragment masses with an *in silico* fragmentation of capsid polyprotein precursor (NCBI: NP_620563) amino acids 256 to 312 (which corresponds to the putative VP4 in other cripaviruses (Czibener et al., 2000) allowed us to unambiguously assign the internal sequences VTGVVGGVADAVKGFF and GKYADPLVGIGNGLTGLLSALG to the putative VP4 protein (Fig. 6). In addition to the 33 b ions shown in Fig. 6, 33 y ions and several *a* and *z* ions were assigned (data not shown). The determination of the two sequences as well as the determination of 5502.5 Da as the intact mass of the protein unambiguously identified the previously undetected TrV small capsid protein VP4.

A salient feature common to several PVs is the hydrophobic character of the VP4 protein, which plays a key role during virus maturation, cell attachment and RNA internalization. In both PVs and HRVs, the P1 polyprotein precursor containing all the capsid protein sequences is myristoylated at its N-terminus (Chow et al., 1987). Cleavage of P1 by the viral 3CD protease produces the capsid proteins VP1 and VP3 and the immature capsid protein myristoyl-VP0. Upon RNA binding, processing of myristoyl-VP0 yields myristoyl-VP4 and VP2. This process seems to be autocatalytic, dependent only on the capsid proteins themselves and probably the viral RNA, and it needs to be accomplished in order to make a mature infective virion (Hogle, 2002; Lee et al., 1993). However, in cripaviruses VP4 is not at the N-terminus of the structural polyprotein, and so the enzyme n-myristoyltransferase cannot attach this highly hydrophobic, saturated fatty acid to the beginning of VP4 (Liljas et al., 2002), which reduces the effectiveness of its membrane interaction function. This observation was experimentally verified with our MS CID fragmentation study of the VP4 protein. In fact, the high number of fragments detected and their coincidence with the theoretical masses from *in silico* fragmentation allowed us to discard any products that resulted from myristoylated VP4 with an expected mass increase of about 210 Da.

Conclusions

In this study we report an improved method that gives high yields of TrV particles from insect feces. This purification protocol also allows for the separation of empty viral particles from full ones. By using an adequate electrophoresis system together with MS analysis, we were also able to resolve the previous uncertainty about the amino acid sequence of TrV's VP4 protein, we established that this peptide is part of the capsid of mature virions, and we measured the stoichiometry of the VP1–VP3 capsid proteins. We verified that empty TrV particles as they appear under TEM are non-infective, that capsid assembly does not depend on interaction with the RNA, and that misprocessing of the precursor protein P1 gives rise to at least seven polypeptides able to assemble into a capsid, but rendering it unable to incorporate the viral RNA. All these results contribute to a better understanding of the TrV viral cycle, and this knowledge provides a contrast with that coming from other similar viral studies.

Eight out of twelve of the currently recognized dicistroviruses are pathogenic to insect pests of agricultural or medical importance; thus they have been postulated to be potential biopesticides (Gordon and Waterhouse, 2006). Due to peculiar biological characteristics like their remarkable mechanism of internal ribosome entry during translation of viral RNA, and their apparent novel mechanism of suppressing host antiviral RNAi systems (Bonning and Miller, 2010), some of the members of this virus family most likely will become model systems for future studies. Recently, we solved the structure of TrV at high

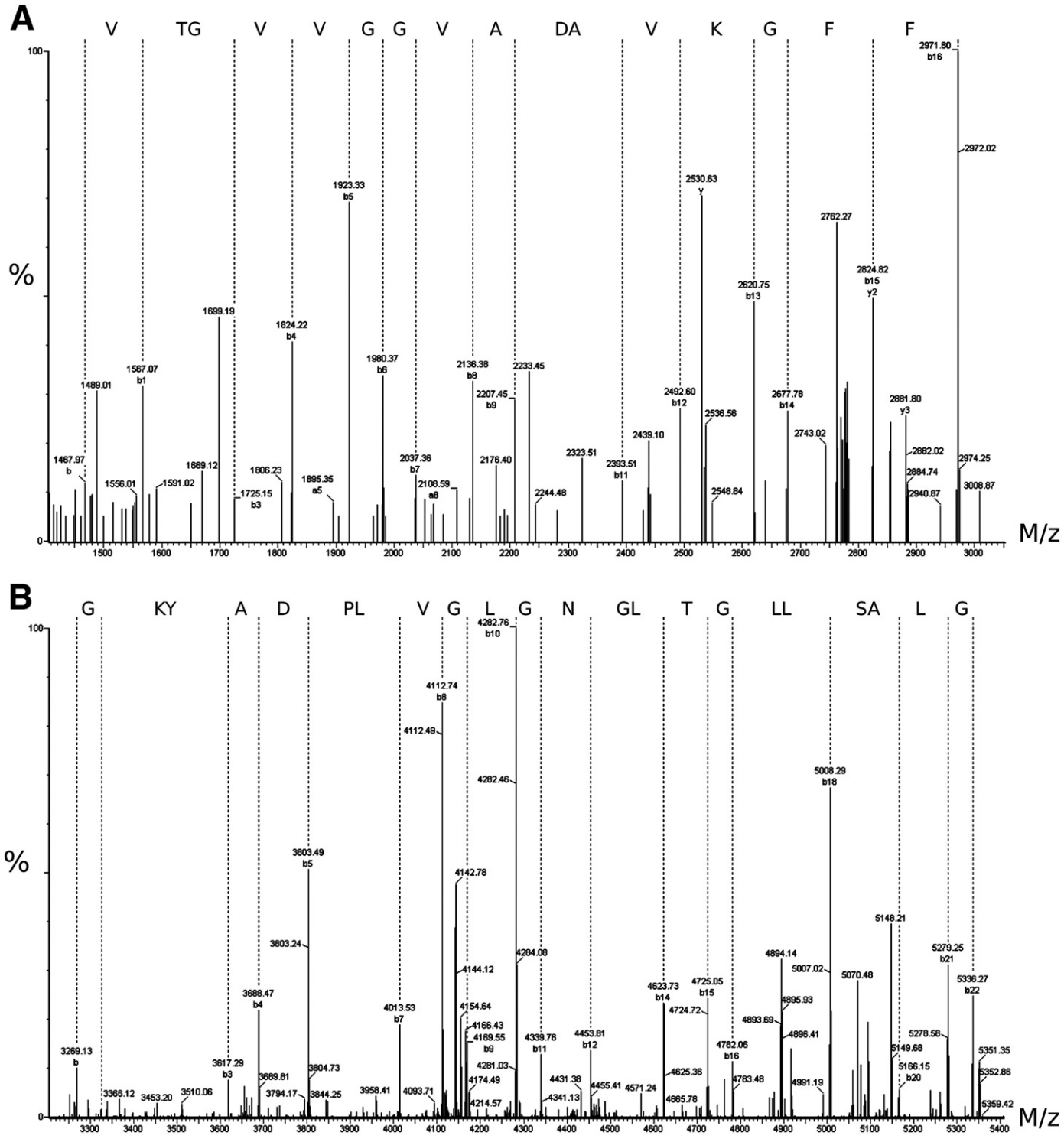

Fig. 6. Identification of the capsid polypeptide precursors' ^{271}V–^{286}F and ^{290}G–^{311}G sequences by top-down sequencing. The $[M+4H]^{+4}$ ion with m/z 1376.8 was CID fragmented and raw spectra were deconvoluted using MaxEnt3 (Waters). Based on an *in silico* fragmentation spectrum of the capsid polyprotein precursor amino acids 256 to 312, ^{271}V–^{286}F and ^{290}G–^{311}G sequences were assigned to the experimentally obtained spectra in A and B, respectively. The dashed lines indicate the assigned b ions and the corresponding amino acid sequence is indicated at the top of the spectrum. L and I amino acids are indistinguishable due to their isobaric nature.

resolution (PDB ID: 3NAP), and now along with the pioneer CrPV structure, the known atomic structures of these two dicistroviruses may contribute to our understanding of the viral cycle at the molecular level. CrPV is the name of the single genus family *Cripavirus* within the *Dicistroviridae* family. Based on phylogenetic distance and the structure of the intergenic region of Acute Bee Paralysis Virus (ABPV), *Aparavirus* is pending for approval by the International Committee on the Taxonomy of viruses as a new genus within this family (Bonning and Miller, 2010). Taking into account that in the phylogenetic tree of the dicistrovirus family TrV belongs to a different branch from that of ABPV and CrPV (Bonning and Miller, 2010), as well as the biological, genetic, and structural knowledge regarding this virus, it is reasonable to propose TrV as the reference for a third *Dicistroviridae* family genus named *Triatovirus*.

Materials and methods

Virus purification

Given that TrV propagation can be accomplished by means of horizontal fecal–oral transmission (Muscio et al., 2000) and that the quantity of virus found in insect feces is relatively high (Rozas-Dennis et al., 2000), it is clear that fully functional and abundant virus can be obtained from TrV-infected insectary colonies. The protocol described here enables the purification of full and naturally occurring empty TrV particles from 'buttons' of dry feces fixed to paper fans inside insectary rearing areas of TrV-infected colonies of *T. infestans* (the papers were stored at room temperature for many months) maintained at the Centro de Estudios Parasitológicos y de Vectores (CEPAVE), La Plata, Argentina. The procedure employed here to extract full and empty TrV particles from feces may also be used with dissected insect intestines as the starting material.

Dry insect feces collected on a Whatman filter were excised from the paper using a standard surgery scalpel until 2 g (weighed using a Sartorius analytical balance) of material was collected. Then, buffer composed of 10 mM NaCl, 1 mM $MgCl_2$ and 200 mM citric acid at pH 6 (Lysis buffer) was added at a ratio of 100 mL per gram of dry material. Phenylmethanesulfonyl fluoride (PMSF, >98.5%, purchased from Sigma) thawed at −20 °C in 2-propanol (Merck, GR for analysis) was added to a final concentration of 1 mM in order to block the activity of serine proteases. A high concentration of buffer was used to prevent eventual acidification of the medium due to the presence of uric acid in the insect feces (Asin and Giojalas, 1995), and pH 6 was chosen to delay PMSF degradation once diluted in water. The mixture was homogenized for 5 min using a vortex mixer and then sonicated using a Sanyo MSE Soniprep 150, operated 10 s ON/10 s OFF for 20 pulses. This sonication step is meant to lyse remaining virus-containing cells, but most importantly to disaggregate the clusters of mixed full and empty particles present in feces to favor the individual migration of both particles in the separation medium. The homogenate was then centrifuged in an Optima L-90K Beckman-Coulter ultracentrifuge for 45 min at 20,000 g_{avg} using a Beckman SW28.1 swinging bucket rotor operated at 12,000 rpm. The collected supernatant was then centrifuged for 2.5 h at 180,000 g_{avg} using a Kontron TFT50.38 fixed angle rotor operated at 40,000 rpm. The resulting pellet was resuspended overnight in 2 mL of 10 mM NaCl, 1 mM $MgCl_2$ and 50 mM Tris–HCl at pH 7.4 (NMT buffer) and then loaded on top of a 35 mL continuous 5%–30% sucrose gradient. The centrifugation was at 100,000 g_{avg} for 3 h in a Beckman SW28.1 rotor. The gradient was fractionated from the bottom to the upper part in 0.5-mL aliquots that were collected in Greiner 96-well Masterblocks and sealed immediately after finishing the process using a silicone-based lid. The gradients were kept in ice in order to prevent thermal diffusion. The individual optical density of each aliquot was then measured at both 260 nm and 280 nm using an Implen Nanophotometer coupled with an LG100 UV-G6786 cell and a lid with a factor of 10 and a light path of 1 mm. A baseline correction was performed using equivalent fractions from a control sucrose gradient. After plotting the absorbance profile, selected aliquots were loaded onto 12.5% polyacrylamide SDS-PAGE gels to check the purity of the samples; DLS measurements were also carried out to check the size of the colloidal particles. As shown in the Results and discussion, two different populations with different protein contents were cleanly separated in the gradient. The one corresponding to the bottom of the gradient, TrV_B, contained mainly full TrV particles, and the one from the upper part of the gradient, named TrV_T, mainly contains empty TrV capsids. After gradient fractionation, equivalent samples were pooled together and dialyzed overnight against 2 L of NMT buffer.

Dynamic light scattering (DLS)

Particle size measurements were carried out using a Zetasizer Nano S (Malvern, UK) DLS, which employs a 5 mW He–Ne laser emitting at $\lambda = 633$ nm and a photomultiplier oriented at 173° from the incident beam. Medium viscosity and refractive index are critical input parameters that can significantly alter the final size estimation due to their evident relationships with light propagation and particle dynamics, respectively. In our case, the different sucrose concentrations present in the different gradient fractions had to be estimated, so for background subtraction a linear relation was assumed between the position of a particular sample in the gradient and its sucrose concentration, with the calculated sucrose concentration being input as a parameter in the DLS software (Malvern, UK).

Volume measurements were performed by loading 65 μL of selected gradient samples in Eppendorf low-volume Uvette plastic cuvettes, and the data shown represent the hydrodynamic diameter of each population *versus* the percentage of the total dispersant volume. For each result, the equipment automatically performed 12 independent measurements.

SDS-PAGE and protein quantification by densitometry

A total of 2.5 μL of each sample was treated with 7.5 μL of 3× loading buffer containing 150 mM Tris–HCl at pH 6.8, 6% SDS, 30% glycerol, 37.5 mM EDTA and 0.06% bromophenol blue and boiled for 5 min at 95 °C. β-mercaptoethanol (3%) was also incorporated into earlier tests, but the results showed no difference from those obtained in its absence. Due to the different molecular masses of the three larger proteins (around 30 kDa) *versus* the smaller VP4, which was predicted to have a mass of no more than 5.6 kDa, an *ad-hoc* separation method was selected to visualize all the capsid proteins in the same gel, thus permitting a densitometric analysis of all the proteins for stoichiometric determination. The gels were 7.2 cm high, being composed of a 1.5-cm resolving portion (bottom part), a 4.5-cm spacer region (middle part) and 1.2 cm of stacking gel (upper part). The resolving gel was composed of 10% glycerol (to enhance the sharpness of lower molecular weight bands), 0.1% SDS, 15% acr./bisacr. (48:3, both purchased from Sigma) and 1 M Tris at pH 8.9. The spacer gel was composed of 0.1% SDS, 15% acr./bisacr. (37.5:1, Bio-Rad) and 0.5 M Tris–HCl at pH 8.9. The stacking gel was composed of 0.1% SDS, 4.7% acr./bisacr. (37.5:1, Bio-Rad) and 0.1 M Tris–HCl at pH 6.8. The gels were run (anode buffer: 0.2 M Tris, pH 8.9, cathode buffer: 0.1 M Tris, 0.1 M Tricine, 0.1% SDS, pH 8.25) at 30 V until the front entered the spacer portion (due to the poor stacking capabilities of Tricine: Schägger, 2006), and then the voltage was switched to 90 V, with a complete run time of 3.5 h. The front always exited the gels before removing the electric field.

For checking sample purity (i.e., characterizing and separating higher weight TrV capsid proteins), standard and more convenient SDS-PAGE gels were used. After several tests, we found that 12.5% was the best concentration to achieve VP0–VP3 identification.

Gels stained with Coomassie blue (for quantitative analysis) were scanned using a Bio-Rad GS-800 densitometer, and the individual protein bands were quantified using ImageJ (Abramoff et al., 2004) and by performing a background baseline subtraction and integrating the optical density (IOD) of each resolved band as a separate entity. To scale the results and make them comparable, the IOD from each band was divided by the number of Coomassie-binding amino acids, yielding a proportional density. In particular, VP1 has 46 Coomassie-binding amino acids (His: 2, Arg: 12, Phe: 15, Tyr: 15, Trp: 2), while VP2 has 39 (His: 8, Arg: 8, Phe: 18, Tyr: 3, Trp: 2), VP3 has 51 (His: 4, Arg: 12, Phe: 16, Tyr: 16, Trp: 3) and VP4 has 4 (His: 0, Arg: 0, Phe: 3, Tyr: 1, Trp: 0). The OD values for the VP1–VP3 bands were integrated together due to insufficient separation, and so their respective numbers of Coomassie-binding residues were added.

Infectivity tests of empty TrV capsids

In order to test the infectivity of TrV capsids, we ran experimental infections by intra-hemocoelically inoculating four groups of healthy

adult *T. infestans* insects, each group containing ten insects (n = 10), and in all cases using 3 μL of inoculant. As a positive control we used TrV purified in a CsCl gradient following the protocol established by Muscio, et al. (1988). We preferred to use this inoculum instead of a TrV_B fraction since the positive infectivity of this viral extract can be considered as a standard. The virus concentration was estimated at 0.33 mg mL^{-1} using the same method employed by these authors. As an empty TrV capsid inoculum we used a concentrated sample from the TrV_T gradient region. The sample was concentrated using a Centricon (10 kDa-CO; Millipore) filter to up to 0.33 mg/mL of protein, as estimated by the BCA method (Smith et al., 1985) with a BCA Protein Assay Kit (Pierce). To evaluate the possible toxicity of NMT buffer to the insects, we also inoculated another group of individuals with this buffer solution. Additionally, in order to estimate the injury to the insects produced by the inoculation treatment, and to have a reference as a negative control, we injected a fourth insect group with sterile saline solution (SSS). Aliquots of 3 μL of the above-mentioned solutions were injected into the insects' hemocoele (Rozas-Dennis et al., 2008). All tested insects were observed for 10 days after inoculation in order to detect TrV infection symptoms like paralysis and death, and to calculate insect survival at the experiment's end. The percentage mortality due to TrV infection was corrected with Abbott's formula (Abbott, 1925):

$$\text{Corrected Mortality}(\%) = \frac{(\%\ \text{live insect control} - \%\ \text{live insect treated})}{(\%\ \text{live insect control})} \times 100.$$

In gel digestion

Gel bands were cut from Coomassie-stained polyacrylamide SDS-PAGE electrophoresis gels and subjected to in-gel tryptic digestion according to Shevchenko et al., 1996, with minor modifications. The gel piece was swollen in digestion buffer containing 50 mM NH_4HCO_3 and 12.5 ng/μL of trypsin (Roche Diagnostics, recombinant, proteomics grade Trypsin, Penzberg, Germany) in an ice bath. After 30 min, the supernatant was removed and discarded, 20 μL of 50 mM NH_4HCO_3 was added to the gel piece and the digestion was allowed to proceed at 37 °C overnight.

Sample preparation for MALDI TOF analysis

Recovered peptides from in-gel digestion were purified prior to MALDI analysis with homemade nano-columns as described by Gobom et al. (1999) with some modifications. A column consisting of 100–300 nL of POROS R2 material (PerSeptive Biosystems, Framingham, MA) was equilibrated with 0.1% TFA, and the bound peptides were subsequently eluted directly onto the MALDI target with 0.5 μL CHCA solution (20 μg/μL in ACN, 0.1% TFA, 70:30, vol/vol). A 1-mL syringe was used to force liquid through the column by applying air pressure.

Mass spectrometric analysis

Peptide mass fingerprinting was performed on a Bruker Autoflex III TOF/TOF mass spectrometer (Bruker-Daltonics, Bremen, Germany). Positively charged ions were analyzed in reflectron mode. The spectra were obtained by randomly scanning the sample surface. Internal calibration was performed from the acquired spectra using trypsin auto digestion peaks achieving less than 30 ppm of mass accuracy. Protein identification was performed in a non-redundant NCBI protein database using the Mascot search engine (http://www.matrixscience.com). The following parameters were used for database searches: missed cleavages = 1; allowed modifications = carbamidomethylation of cysteine (complete) and oxidation of methionine (partial). MALDI TOF/TOF analysis of the selected VP4 tryptic peptide was performed by acquiring 2000 laser shots. The tolerances for precursor ions and fragment ions used for database searching analysis were 30 ppm and 0.7 Da, respectively.

Intact mass determination and top-down protein sequencing

A total of 80 μg of full TrV virus was precipitated with the 2-D Clean-Up Kit (GE Healthcare). The protein pellet was partially resuspended in 30 μL acetonitrile, 0.2% formic acid. Since the resuspension was not complete, 30 μL 0.2% formic acid in water was added and the supernatant solution was directly injected into a Q-Tof Micro (Waters) mass spectrometer. Mass spectra were manually acquired in the 700–2500 m/z range. Protein intact mass was determined with MaxEnt1 software (Waters) using the deconvolution default parameters. Mass ranges were selected based on available protein sequence information (NCBI: NP_620563), and the software was set to iterate to convergence. To assign a test sequence for the putative TrV VP4 protein, a fragment of 56 amino acids starting with the quartet AGKE was selected (see Results and discussion). For top-down protein sequencing, the $[M+4\,H]^{+4}$ ion with m/z 1376.8 was selected for CID fragmentation. Collision energies from 25 to 32 eV were used and the spectra were deconvoluted using MaxEnt3 software (Waters). Masses obtained experimentally were matched with an *in silico* fragmentation pattern of the sequence corresponding to the putative TrV VP4 protein using the PepSeq computational tool (Waters).

Transmission electron microscopy (TEM)

TEM images were acquired using a Phillips EM208S transmission electron microscope (nominal resolution of 0.34 nm) combined with a Morada camera. Uranyl acetate (2%) was used for staining, and the TrV solutions used for TEM studies were at a concentration lower than 0.1 mg mL^{-1} (protein). The samples were mounted on carbon-coated copper grids previously polarized by the glow-discharge method.

N-terminal sequencing of VP0 and non-canonical capsid proteins

Purified TrV capsids from the TrV_T fraction (see *Virus purification*) were subjected to 15% SDS-PAGE (Laemmli, 1970) and then blotted onto a PVDF membrane using a Bio-Rad Trans-Blot SD for 45 min at 15 V. The membrane was stained with Coomassie brilliant blue. VP0 and PP4 bands were excised from the membrane and subjected to Edman degradation in a PROCISE-cLC (Applied Biosystems). Four residues at the N-terminus of each polypeptide/s were sequenced. The other non-canonical proteins did not transfer properly and thus we could not perform the analysis.

Acknowledgments

This work was partially supported by the MICINN, the Basque Government (Etortek Research Program 2008/2010), Bizkaia:Xede and Bizkaia County, Spain. The authors are grateful to Dr. Dieter Blaas from the Max F. Perutz Laboratories, Medical University of Vienna, for providing the sample of denatured HRV2; to the Plataforma de Proteòmica, Parc Cientific de Barcelona for N-terminal sequencing (member of the Proteored network); to the Servicio Nacional de Chagas, Córdoba, Argentina for the gift of *T. infestans* colonies; to Dr. Augusto Bellomio and Dr. Ana Rosa Viguera at the Unidad de Biofísica for useful advice and support; and to Sonia López for additional experimental support. Dr. Agirre's work was supported by a UPV/EHU contract (UPV-IT-461-07). Dr. Marti is researcher of the CONICET, Argentina. Dr. Guérin is partially

supported by Bizkaia:Xede association and MICINN. The Servicio General de Proteómica-SGiker of the University of the Basque Country is a member of the Proteored network, and is supported by UPV/EHU, MICINN, GV-EJ and ESF agencies.

References

Abbott, W.S., 1925. A method of computing the effectiveness of an insecticide. J. Econ. Entomol. 18, 265–267.

Abramoff, M.D., Magelhaes, P.J., Ram, S.J., 2004. Image processing with ImageJ. Biophotonics International 11, 36–42.

Asin, S.N., Giojalas, L.C., 1995. Type of rectal contents and infectivity of domiciliary populations of *Triatoma infestans* (Hemiptera: Reduviidae) in Argentina. J. Med. Entomol. 32 (4), 399–401.

Basavappa, R., Syed, R., Flore, O., Icenogle, J.P., Filman, D.J., Hogle, J.M., 1994. Role and mechanism of the maturation cleavage of VP0 in poliovirus assembly: structure of the empty capsid assembly intermediate at 2.9 Å resolution. Protein Sci. 3, 1651–1669.

Bonning, B.C., Miller, W.A., 2010. Dicistroviruses. Annu. Rev. Entomol. 55, 129–150.

Brabec, M., Schober, D., Wagner, E., Bayer, N., Murphy, R.F., Blaas, D., Fuchs, R., 2005. Opening of size-selective pores in endosomes during human rhinovirus serotype 2 in vivo uncoating monitored by single-organelle flow analysis. J. Virol. 79, 1008–1016.

Ceres, P., Zlotnick, A., 2002. Weak protein–protein interactions are sufficient to drive assembly of hepatitis B virus capsids. Biochemistry 41 (39), 11525–11531.

Chow, M., Newman, J.F.E., Filman, D., Hogle, J.M., Rowlands, D.J., Brown, F., 1987. Myristylation of picornavirus capsid protein VP4 and its structural significance. Nature 327, 482–486.

Czibener, C., La Torre, J.L., Muscio, O.A., Ugalde, R.A., Scodeller, E.A., 2000. Nucleotide sequence analysis of Triatoma virus shows that it is a member of a novel group of insect RNA viruses. J. Gen. Virol. 81, 1149–1154.

Czibener, C., Alvarez, D., Scodeller, E., Gamarnik, A., 2005. Characterization of internal ribosomal entry sites of Triatoma virus. J. Gen. Virol. 86 (8), 2275–2280.

Estrozi, L.F., Neumann, E., Squires, G., Rozas-Dennis, G., Costabel, M., Rey, F.A., Guérin, D.M.A., Navaza, J., 2008. Phasing of the Triatoma virus diffraction data using a cryo-electron microscopy reconstruction. Virology 375 (1), 85–93.

Gobom, J., Nordhoff, E., Mirgorodskaya, E., Ekman, R., Roepstorff, P., 1999. Sample purification and preparation technique based on nano-scale reversed-phase columns for the sensitive analysis of complex peptide mixtures by matrix-assisted laser desorption/ionization mass spectrometry. J. Mass Spec. 34, 105–116.

Gordon, K.H., Waterhouse, P.M., 2006. Small RNA viruses of insects: expression in plants and RNA silencing. Adv. Virus Res. 68, 459–502.

Hogle, J.M., 2002. Poliovirus cell entry: common structural themes in viral cell entry pathways. Annu. Rev. Microbiol. 56, 677–702.

Iwasaki, K., Trus, B.L., Wingfield, P.T., Cheng, N., Campusano, G., Rao, V.B., Steven, A.C., 2000. Molecular architecture of bacteriophage T4 capsid: vertex structure and bimodal binding of the stabilizing accessory protein, Soc. Virology 271 (2), 321–333.

Jacobson, M.F., Baltimore, D., 1968. Polypeptide cleavages in the formation of poliovirus proteins. Proc. Natl. Acad. Sci. 61 (1), 77–84.

Johnson, J.M., Jinghua, T., Nyame, Y., Willits, D., Young, M.J., Zlotnick, A., 2005. Regulating self-assembly of spherical oligomers. Nano Lett. 5 (4), 765–770.

Laemmli, U.K., 1970. Cleavage of structural proteins during the assembly of the head of bacteriophage T4. Nature, 227.

Lee, W.M., Monroe, S.S., Rueckert, R., 1993. Role of maturation cleavage in infectivity of Picornaviruses: activation of an infectosome. J. Virol. 67, 2110–2122.

Liljas, L., Tate, J., Lin, T., Christian, P., Johnson, J.E., 2002. Evolutionary and taxonomic implications of conserved structural motifs between picornaviruses and insect picorna-like viruses. Arch. Virol. 147, 59–84.

Marti, G.A., Gonzalez, E.T., García, J.J., Viguera, A.R., Guérin, D.M.A., Echeverria, M.G., 2008. AC-ELISA and RT-PCR assays for diagnosis of Triatoma virus (TrV) in triatomines (Hemiptera: Reduviidae) species. Arch. Virol. 153 (8), 1427–1432.

Moore, N.F., Kearns, A., Pullin, J.S.K., 1980. Characterisation of cricket paralysis virus-induced polypeptides in Drosophila cells. J. Virol. 33, 1–9.

Muscio, O.A., La Torre, J.L., Scodeller, E.A., 1987. Small noncclued viruses from bug *Triatoma infestans* (Hemiptera: Reduviidae). J. Inv. Pathol. 49, 218–220.

Muscio, O.A., La Torre, J.L., Scodeller, E.A., 1988. Characterization of Triatoma virus, a Picorna-like virus isolated from the Triatomine bug *Triatoma infestans*. J. Gen. Virol. 69, 2929–2934.

Muscio, O.A., La Torre, J.L., Bonder, M., Scodeller, E.A., 1997. Triatoma virus pathogenicity in laboratory colonies of *Triatoma infestans* (Hemiptera: Reduviidae). J. Med. Entomol. 34, 253–256.

Muscio, O.A., Bonder, M., La Torre, J.L., Scodeller, E.A., 2000. Horizontal transmisión of Triatoma virus through the fecal–oral route in *Triatoma infestans*. J. Med. Entomol. 37 (2), 271–275.

Rossmann, M.G., Tao, Y., 1999. Structural insight into insect viruses. Nat. Struct. Biol. 6, 717–719.

Rowlands, D.J., Sanga, D.V., Brown, F., 1975. A comparative chemical and serological study of the full and empty particles of foot-and-mouth disease virus. J. Gen. Virol. 26, 227–238.

Rozas-Dennis, G.S., Cazzaniga, N.J., 2000. Effects of Triatoma virus (TrV) on the fecundity and moulting of *Triatoma infestans* (Hemiptera: Reduviidae). Ann. Trop. Med. Parasitol. 94, 633–641.

Rozas-Dennis, G.S., La Torre, J.L., Muscio, O.A., Guérin, D.M.A., 2000. Direct methods for detecting Picorna-like virus from dead and alive triatomine insects. Mem. Inst. Oswaldo Cruz 95 (3), 323–327.

Rozas-Dennis, G.S., Cazzaniga, N.J., Guerin, D.M.A., 2002. *Triatoma patagonica* (Hemiptera, Reduviidae), a new host for Triatoma virus. Mem. Inst. Oswaldo Cruz 97 (3), 427–429.

Rozas-Dennis, G.S., Squires, G., Pous, J., Costabel, M.D., Lepault, J., Navaza, J., Rey, F.A., Guérin, D.M.A., 2004. Purification, crystallization and preliminary X-ray analysis of Triatoma virus (TrV) from *Triatoma infestans*. Acta Cryst. D60, 1647–1650.

Rozas-Dennis, G.S., Marti, G.A., Guérin, D.M.A., 2008. Protocolo de inoculación intrahemocélica en vinchucas. http://www.redtrv.org/Protocolos2008.

Rweyemamu, M.M., Terry, G., Pay, T.W.F., 1979. Stability and immunogenicity of empty particles of foot-and-mouth disease virus. Arch. Virol. 59, 69–79.

Salunke, D.M., Caspar, D.L.D., Garcea, R.L., 1989. Polymorphism in the assembly of polyomavirus capsid protein VP1. Biophys. J. 56, 887–900.

Schägger, H., 2006. Tricine–SDS-PAGE. Nat. Prot. 16 (1).

Schmitz, K.S., 1990. An Introduction to Dynamic Light Scattering by Macromolecules. Academic Press, San Diego, p. 22.

Shevchenko, A., Wilm, M., Vorm, O., Mann, M., 1996. Mass spectrometric sequencing of protein from silver-stained polacrylamide gels. Anal. Chem. 68 (5), 850–858.

Siber, A., Podgornik, R., 2007. Role of electrostatic interactions in the assembly of empty spherical capsids. Phys. Rev. E 76, 061906.1–061906.10.

Smith, P.K., Krohn, R.I., Hermanson, G.T., Mallia, A.K., Gartner, F.H., Provenzano, M.D., Fujimoto, E.K., Goeke, N.M., Olson, B.J., Klenk, D.C., 1985. Measurement of protein using bicinchoninic. Anal. Biochem. 150, 76–85.

Squires, G., Pous, J., Rozas-Dennis, G.S., Costabel, M.D., Agirre, J., Marti, G., Navaza, J., Guérin, D.M.A., Rey, F.A., in preparation. The crystallographic structure of Triatoma virus (TrV) highlights the Dicistroviridae and Picornaviridae family differences.

Tate, J., Liljas, L., Scotti, P., Christian, P., Lin, T., Johnson, J.E., 1999. The crystal structure of cricket paralysis virus: the first view of a new virus family. Nat. Struct. Biol. 6 (8), 765–774.

Tuthill, T.J., Bubeck, D., Rowlands, D.J., Hogle, J.M., 2006. Characterization of early steps in the poliovirus infection process: receptor-decorated liposomes induce conversion of the virus to membrane-anchored entry-intermediate particles. J. Virol. 80, 172–180.

Williamson, C., Rybicki, E.P., Kasdorf, G.G.F., Von Wechmar, M.B., 1988. Characterization of a New Picorna-like Virus Isolated from Aphids. J. Gen. Virol. 69, 787–795.

WHO—World Health Organization, 2002. Control of Chagas disease. Second Report from the Committee of Experts. : Series of Technical Reports 905Geneva, Switzerland. 117 pp.